Tellus (1984), *36A*, 120–131

A two-dimensional, seasonal, energy balance climate model with continents and ice sheets: testing the Milankovitch theory

ROBERT G. WATTS, *Department of Mechanical Engineering, Tulane University, New Orleans, Louisiana 70118, U.S.A.*, and Md. EHTESHAMUL HAYDER, *School of Mechanical Engineering, Princeton University, Princeton, New Jersey, U.S.A.*

(Manuscript received November 17, 1982; in final form March 27, 1983)

ABSTRACT

A simple seasonal, two-dimensional, energy balance climate model that contains an ice sheet model is forced by varying the orbital parameters. If a mechanism that enhances melting during ice sheet retreat is introduced, variations in ice volume resembling those deduced from oxygen isotope variations are predicted. Since the Milankovitch theory asserts that cool high latitude summers lead to the growth of ice sheets, a seasonal climate model with continents must be used to test the theory. An ice sheet model must also be included because the presence of an ice sheet leads to a large amplification of its own size. When all three of these ingredients are present in the model, very large ice sheets can be produced. A strong 100 kyr cycle is present only if a mechanism that enhances ice sheet collapse is introduced. Other predicted features of past climate variations, such as ocean temperature and sea ice variation, also resemble paleoclimate reconstructions from proxy data.

1. Introduction

Oxygen isotope data from deep ocean cores suggest that global land ice volume has undergone large oscillations during the last 700–1000 kyr. Spectral analyses of these data indicate a very strong spectral peak with a period of approximately 100 kyr and weaker peaks near 40 kyr and 20 kyr (Hays et al., 1976). According to the astronomical theory of ice ages (Milankovitch, 1941), the periodic advance and retreat of the Northern Hemisphere ice sheets was caused by changes (mostly in the seasonal variation) of the high latitude solar radiation due to perturbations in the Earth's orbital parameters. The 20 kyr and 40 kyr spectral peaks in the oxygen isotope data are well correlated with the high latitude summer insolation variations. However, the 100 kyr spectral peak, which is the strongest of the oxygen isotope peaks, is essentially absent from the spectral analysis of the high latitude summer insolation (Birchfield et al., 1981).

Although the astronomical theory of ice ages has recently gained many proponents, climate models have generally failed to predict the large ice sheet advances that are known to have occurred during the Quaternary (Pollard, 1980; North and Coakley, 1979; Suarez and Held, 1979). Specifically, the large 100 kyr cycle is not predicted by climate models. Recently, however, Pollard (1982), Birchfield et al. (1981), and Oerlemans (1980) have obtained encouraging results from simple ice sheet models by including bedrock sinking and a crudely parameterized ice calving mechanism. These models were not, however, driven by climate models. Instead, the ice sheets were forced by assuming that the latitudinal position of the permanent snow line responds linearly to the summer insolation anomaly at some fixed latitude. The latitude used, as well as the amplitude of the signal, were somewhat arbitrarily chosen. Birchfield (1977) suggested earlier that the nonlinear response of the ice sheets themselves might be responsible for the appearance of the 100 kyr cycle.

According to the Milankovitch hypothesis, ice ages are initiated by cool high latitude summers which prevent the complete melting of continental ice. It has been suggested many times that the location of continents near the poles is a necessary condition for the initiation of glacial cycles (Tanner, 1968; Burrett, 1982). Some previous energy balance climate models have included a latitudinal variation of land fraction. Suarez and Held (1979) studied a two-level energy balance model in which land and sea surfaces were treated differently in the surface energy balance, but where the atmospheric temperature was treated as a zonally averaged quantity. North and Coakley (1979) experimented with a seasonal model in which the atmospheres above land and sea were each zonally averaged and were allowed to communicate energetically through a convective mechanism. They used a land fraction that was independent of latitude, however. Barron et al. (1981) included some of the effects of land distribution in an energy balance model by including land fraction within the zonally averaged thermal inertia. They did not, however, distinguish between land and sea temperatures in any direct way. North et al. (1982) recently studied the effects of continentality on the response of the seasonal cycle to orbital perturbations and found qualitative agreement with the Milankovitch hypothesis. Their model did not contain ice sheets, however, and therefore could not be used to investigate the Milankovitch hypothesis directly.

In order to properly model the effect of changing orbital parameters on climate, a climate model should contain at least the effects of seasonality, the distribution of continents, and the dynamics of ice sheet growth and collapse. Seasonality must be included because, according to Milankovitch, ice ages are initiated when cool high latitude summers lead to the persistence of snow on land during the entire year. The distributions of land and sea are important because they affect the seasonal temperature range. If, as Birchfield (1977) has suggested, the presence of an ice sheet itself leads to the appearance of the 100 kyr cycle, then the ice sheet should be included also. We will show that the presence of the ice sheet also leads to a large amplification of its own size.

The model that we have used consists of two parts: a two-dimensional (latitude and longitude) model of the atmosphere with an interactive ocean mixed layer, and a dynamical model of the ice sheet. Horizontal transport of energy is modeled as a linear diffusion process following North (1975), and infrared cooling is modeled as a linear function of surface temperature following Budyko (1969). The model has one central group of continents and one ocean. The configuration is shown in Fig. 1. The land fraction at any latitude is estimated by a least square error technique using realistic land fraction as it exists today. The mid-continent is set at longitude (ϕ) equal to 0° and the mid-ocean at longitude equal to 180°. Owing to the assumed symmetry of distribution, the actual computation is based on $\phi = 0°$ to 180°.

The model climate is forced by allowing the orbital parameters (obliquity, precession, and eccentricity) to vary. The effects of these parameters on the distribution of the incident solar flux is computed from the formulae given by Berger (1978). The computation is made for the last two glacial cycles (about 240,000 YBP to present). Antarctica (the continent located at the south pole) is assumed to be covered by a permanent icecap.

The ice sheet model follows those of Weertman (1976) and Birchfield (1977). It is allowed to grow from the poleward edge of the Northern Hemisphere continent. Glaciation initiates on an initially ice free continent if the snowline remains on the land over the whole year. While it would be most desirable that the ice sheet model be contained explicitly within the climate model, we found that running the models as they are presently formulated in that way was very time consuming and expensive. We expect to undertake that task in the

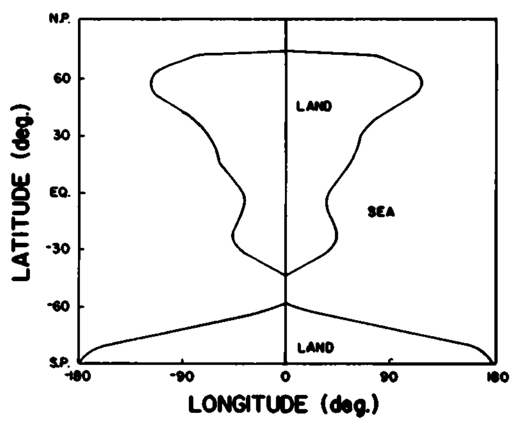

Fig. 1. Model land/sea distribution.

future. For the present, however, we feel that combining the climate and ice sheet models in a somewhat looser way can serve to guide future numerical experiments while perhaps generating some interesting, if preliminary, results. We therefor proceeded by using the climate model to obtain the position of the mid-summer, mid-continent snow line for 23 selected times during the last 240,000 years. We found that we could match this data with a linear function of the insolation anomoly at 73° N. This was done solely in order to have a smooth function as an input to the ice sheet model. The snow line signal obtained from the climate model matches the insolation signal (at 73° N) very well. Other models make no attempt to relate insolation anomolies that are used to drive ice sheet models to a signal computed using a climate model. For example, Oerlemans (1980) used a simple sine wave function, as did Birchfield (1977), while Weertman (1976) used the summer half-year insolation anomaly at 50° N and Pollard (1982) used that at 55° N. Birchfield et al (1981) used the insolation anomaly at 60° N.

The fact that the ice sheet is not explicitly contained within the climate model creates another problem, however. While the climate model contains snow co-albedo feedback, it does not contain the additional ice co-albedo feedback created by the presence of the ice sheet. This is especially important in the summer when snow would recede, but the ice sheet does not. In addition, the fact that the ice sheet extends high above sea level actually decreases the amount of infrared radiation leaving the earth, as pointed out by Bowman (1982). In Section 5, we briefly explore the consequences of leaving these feedbacks out of our model.

In the following sections we briefly describe the climate and ice sheet models. More detailed descriptions of the models and of the solution techniques are contained in Hayder (1982).

2. The atmosphere–ocean model

The transient energy equation that we use is well known. The rate of change of stored energy in a column from the top of the atmosphere to the bottom of the ocean mixed layer or the layer below the land surface across which negligible vertical energy exchange takes place is equal to the net radiant energy in through the top of the atmosphere minus the divergence of the horizontal heat flux due to atmospheric and oceanic transport. We use the seasonal climate model to determine the location of the latitudinal position of the snow line. Seasonality is affected by the heat capacity of the upper layer of the ocean, but not by the deep ocean. The deep ocean probably affects climate on time scales ranging from several hundred to a few thousand years. This time scale is intermediate to the seasonal cycle and the Milankovitch cycles. Recent evidence (Schnitker, 1983) indicates that its effect can be detected in the deep sea record. It seems likely, however, that these effects will appear as perturbations on the Milankovitch cycles. At this stage in the modeling process, it seems wise to neglect them.

The transient energy equation can now be written in the following form:

$$a(x,T)\,S(x,t)\,Q-(A+BT)+\nabla\cdot D\nabla T = C(x,\phi)\frac{\partial T}{\partial t}. \qquad (1)$$

$A + BT$ is the infrared radiation leaving the top of the atmospheric column. Q is the solar constant divided by four. $a(x, T)\ QS(x, t)$ is the solar radiation absorbed by the system, where $a(x, T)$ is the co-albedo and $S(x, t)$ is a distribution term computed from the formulation by Berger (1978). $\nabla\cdot D\nabla T$ is a diffusion term, as used, for example, by North (1975). $C(x, \phi)$ is the local heat capacity. T is temperature in degrees centigrade and t is time. x is the sine of the latitude and ϕ is the longitude.

Eq. (1) is nonlinear because the co-albedo depends on latitude, longitude and local temperature. It is usually assumed (North et al., 1981) that the co-albedo varies as follows:

$$\begin{aligned} a &= a_0 + a_2 P_2(x), \quad && x < x_1 \\ &= b_0, && x > x_1 \end{aligned} \qquad (2)$$

where x_1 is the sine of the latitude poleward from which the land or sea is snow or ice covered and $P_2(x)$ is the second Legendre polynomial. In order to allow for differences between land and sea co-albedo we will use different values of a_0, a_2, b_0, and x_1 for land and sea. These are designated as a_{01}, a_{21}, b_{01}, and x_1 for the land and a_{0s}, a_{2s}, b_{0s}, and x_s for the sea.

In order to partially account for oceanic heat transport, we have used a diffusion coefficient of the form $D = D_{avg} + \Delta D \cos\phi$. The diffusion coefficient therefore varies between $D_{avg} - \Delta D$ in mid-ocean and $D_{avg} + \Delta D$ at mid-continent.

When ice sheet dynamics are included with the climate model, two additional effects must be considered that are not included in eq. (1). The temperature of the atmosphere just above an ice sheet is lower than the mean sea level temperature because the atmospheric temperature decreases with height. The temperature difference between the surface of the ice sheet and mean sea level can be approximated by the local temperature lapse rate, Γ, times the local height, h. The decrease in infrared radiation due to this temperature difference is $B\Gamma h$. The effect of ice sheet height is included in the model by adding $B\Gamma h_{avg}$ to the left hand side of eq. (1) in regions where an ice sheet is present. h_{avg} is the average height of the ice sheet.

Ice sheet melting produces cold fresh water which covers the sea surface near the edge of a melting ice sheet. The model assigns a sea cooling effect to the ocean surface between 40° N and 55° N whenever Northern Hemisphere ice sheets are melting. If $\dot{m}''$ is the mass rate of ice melt per unit area of sea surface within the specified region, then the sea cooling per unit surface area is assumed to be the latent heat times $\dot{m}''$. $\dot{m}$ is calculated from the ice sheet model, and $\dot{m}''$ is obtained by dividing by the area of the sea surface in the indicated region. $\dot{m}''$ times the latent heat is then added to the left hand side of eq. (1). In performing the actual calculation, both these new terms are combined with $aQS(x) - A$. The first term on the left hand side of eq. (1) is replaced by

$$F(x, \phi, t) = a(x, T)\, S(x, t)\, Q + B\Gamma h_{avg} - \dot{m}''\mathcal{L} - A \tag{3}$$

The solution of eq. (1), with the co-albedo variation given by eq. (2) and with the function $F(x, \phi, t)$ replacing $aQS(x, t)$, is accomplished by an iterative technique. The temperature is represented as a series of the form

$$T(x, \phi, t) = \sum_n \sum_m A_{nm}(t) \cos(m\phi)\, P_n^m(x), \tag{4}$$

where $P_n^m(x)$ are associated Legendre polynomials and $A_{nm}(t)$ are undetermined functions of time. This form is substituted into eq. (1) and the resulting equation multiplied by $P_r^s(x)\cos(s\phi)$ and integrated over the sphere. There results a set of equations

$$\begin{aligned}
&\int_0^\pi \int_{-1}^1 F(x, \phi, t)\, P_r^s(x) \cos(s\phi)\, dx\, d\phi \\
&- \int_0^\pi \int_{-1}^1 \sum_n \sum_m [B + D_{avg}\, n(n+1)]\, P_n^m(x)\, P_r^s(x) \\
&\times \cos(m\phi) \cos(s\phi)\, dx\, d\phi \\
&- \int_0^\pi \int_{-1}^1 \sum_n \sum_m n(n+1)\, \Delta D P_n^m(x)\, P_r^s(x) \\
&\times \cos(\phi) \cos(m\phi) \cos(s\phi)\, dx\, d\phi \\
&= \int_0^\pi \int_{-1}^1 \sum_n \sum_m C(x, \phi)\, P_n^m(x)\, P_r^s(x) \cos(m\phi) \\
&\times \cos(s\phi)\, dx\, d\phi \frac{dA_{nm}}{dt}.
\end{aligned} \tag{5}$$

An initial seasonal variation of $T(x, \phi, t)$ is now assumed. Snow is assumed to be present when $T < -1$ °C over land and sea ice is present when $T < -3.5$ °C over sea. Using this information, the integral involving $F(x, \phi, t)$ can be evaluated, and eqs. (5) can be integrated over one season. The new values of $A_{nm}(t)$, together with eq. (4), establish a new estimate of seasonal temperature. The process is repeated until convergence is indicated.

To obtain reasonable accuracy balanced by manageable computer time, we have kept six terms in eq. (4). These involve $P_0(x)$, $P_1(x)$, $P_2(x)$, $P_1^1(x)$, $P_2^1(x)$, and $P_3^1(x)$. The $P_0(x)$ term gives the global average. The $P_1(x)$ term is an odd term and allows representation of the interhemispheric asymmetry. The $P_2(x)$ term gives the equator to pole zonal average gradient. The last three terms (of which only the second is odd) allow the representation of longitudinal gradients.

3. Validation of the seasonal climate model

The climate model described above has been tested to see whether, with present-day orbital parameters, it can be used to predict seasonal variations similar to those that actually occur. The constants used in the model are listed in Table 1. A and B are nearly the same as those used by North et al. (1981), as is D_{avg}. The value of ΔD allows a mid-ocean diffusion coefficient 15% larger than the zonal average, due to ocean currents. The co-efficients in the land and sea co-albedo formulae

Table 1. *Constants used in the seasonal climate model*

A	208.4	W m^{-2}
B	1.8	W m^{2} C^{-1}
T_0	−10.0	C
a_{0l}	0.70	
a_{2l}	−0.08	
b_{0l}	0.35	
a_{0o}	0.69	
a_{2o}	−0.12	
b_{0o}	0.4	
D_{avg}	0.65	W m^{-2} C^{-1}
$\Delta D/D_{avg}$	−0.15	
Q	345.0	W m^{-2}
Γ	3.5	C km^{-1}

were chosen after examining NOAA satellite data (Winston et al., 1979). The fit to the data was done more or less by eye. Actually computing zonal averages for land and sea portions from the data would be a major undertaking by itself. Our values are, however, close to those used by a number of authors. The value used for the lapse rate, $\Gamma = 3.5$ C km^{-1}, represents that at high latitudes where, especially in winter, the lapse rate is much smaller than the adiabatic lapse rate.

The results are reported in detail by Hayder (1982). As expected, seasonal variations in temperature are larger over the continent than over the ocean. There is less seasonality in the Southern Hemisphere because the ocean fraction is so large. The comparison of seasonal temperature variations at both mid-continent and mid-ocean with present-day values is quite good. In the interest of space, we report here only the comparison of the model generated mid-continent seasonal snow line in the Northern Hemisphere with data of Kukla (1978) in Fig. 2. We refer the interested reader to Hayder (1982) for other comparisons. The seasonal climate model appears to simulate broad aspects of the present climate quite well.

4. The ice sheet model

Atmospheric poleward transport of water vapor results in snow precipitation beyond seasonally variable snow lines. If summer insolation is not sufficient to melt the winter snow accumulation, ice will stay permanently on the continent. The colder climate nourishes the resulting ice sheet. The ice mass flows to maintain some equilibrium shape. Following Weertman (1976), we assume the ice sheet maintains a quasiequilibrium plastic shape such that its height, h, is

$$h = [\gamma(L - y)]^{1/2}, \tag{6}$$

where γ is a constant, y is the distance equatorward from the center of the ice sheet and L is half the latitudinal extent of the ice sheet. The assumed ice sheet is shown in Fig. 3. The portion of the ice sheet lying towards the pole from the plane of freezing temperature (known as the equilibrium line for the two-dimensional representation) can accumulate ice while the equatorward portion ablates. The volume accumulation rate per unit area at any point on the equatorward half of an ice sheet of height h and equilibrium line height h_s has been given by Oerlemans (1980) as

$$\begin{aligned} g &= a(h - h_s) - b(h - h_s)^2, & h - h_s &< a/2b \\ &= a^2/2b, & h - h_s &> a/2b \end{aligned} \tag{7}$$

where a and b are constants. This is very similar to expressions used by Weertman (1976), Pollard (1982) and others.

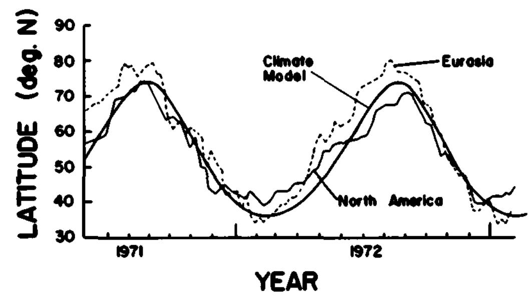

Fig. 2. Comparison of the mid-continent snowline with the data of Kukla (1978).

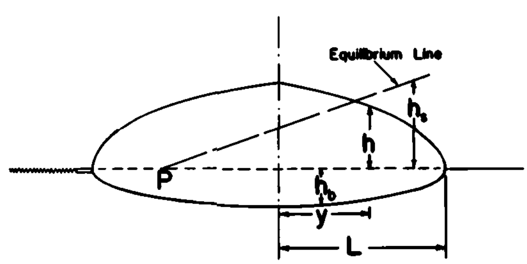

Fig. 3. The model ice sheet.

The weight of an ice sheet causes the underlying bedrock to sink. The sinking is assumed to be represented by a first order lag (after Oerlemans, 1980) with a time constant of 5000 years. Thus, the portion of the ice sheet below ground level is governed by the equation

$$\frac{dh_{b0}}{dt} = \alpha\left(\frac{h_0}{3} - h_{b0}\right), \tag{8}$$

where $h_{b0} = h_b(y = 0)$, h_b being the depth of the ice sheet below the surface, and $h_0 = \sqrt{\gamma L}$. By defining $\eta = h_{b0}/h_b$ and $R = \sqrt{L}$ and assuming that the shapes of ice sheets below and above ground are the same, we can rewrite the above equation as

$$\frac{d\eta}{dt} = \alpha(\tfrac{1}{3} - \eta) - \frac{\eta}{R}\frac{dR}{dt}. \tag{9}$$

The volume balance of the equatorward half of the ice sheet is obtained by integrating the accumulation rate over the equatorward half and setting this equal to the rate of change of the volume of that half of the ice sheet. The result is

$$\frac{d}{dt}\left[\tfrac{2}{3}(1 + \eta)L^{3/2}\right] = \int_0^L g(y)\,dy. \tag{10}$$

Using $R = \sqrt{L}$ we obtain a somewhat more convenient form.

$$2\sqrt{\gamma}(1 + \eta)\frac{dR}{dt} = \frac{1}{R^2}\int_0^L g(y)\,dy - \tfrac{2}{3}\sqrt{\gamma}R\frac{d\eta}{dt} \tag{11}$$

Substituting $d\eta/dt$ from eq. (9) and rearranging gives

$$\frac{dR}{dt} = \frac{1}{2\sqrt{\gamma}(1 + 2\eta/3)}\left[\frac{1}{R^2}\int_0^L g(y)\,dy - \tfrac{2}{3}\sqrt{\gamma}\alpha R(\tfrac{1}{3} - \eta)\right]. \tag{12}$$

Eqs. (9) and (12) are the two working equations for the ice sheet model. The term $\int_0^L g(y)\,dy$ is computed numerically. The height of the equilibrium line h_s is $s(L - P + y)$, where s is the slope of the equilibrium line, dh_s/dy, and P is the point where the equilibrium line reaches sea level, measured from the poleward edge of the continent. P is called the climate point. Values of slope s and climate point P are computed from the seasonal climate model and used for computation of the above integral term.

According to Ruddiman and McIntyre (1981), Mayewski et al. (1981), and many others, the terminations of major glaciations occurred rather suddenly and dramatically over periods of perhaps 5000 to 10,000 years. It would be very difficult to predict such rapid deglaciations with the above model. Indeed, it is generally believed (Ruddiman and McIntyre, 1981) that the rapid deglaciations are associated with process not explicitly modeled by eq. (7). Once an ice sheet is large enough to extend a long distance along an ocean shore, it can lose mass by calving into the sea. If the orbital parameter orientations cause a warming period, rapid deglaciation can be caused by two effects associated with the ocean. First, iceberg calving into the ocean causes a chilling of the midlatitude ocean surface, decreasing evaporation, and thereby starving the ice sheet. This effect should be proportional to the rate at which calving occurs. Ruddiman and McIntyre (1981) report that a reduction of the ocean surface temperature by as much as 10 °C has occurred in certain areas during rapid deglaciations.

The second effect associated with iceberg calving is probably more serious. As calving occurs, the sea level rises, floating the edges of the ice sheet, and causing calving to be even more rapid. Pollard (1982) included an iceberg calving effect in an ice sheet model by setting the mass balance equal to a large negative value at points along the edges of the ice sheet that were exposed to water when the water level was higher than the base of the ice sheet.

Little is known about how to include these effects in such a simple model as that presented here. We have modeled them by simply assuming that the net accumulation rate decreases linearly with the rate of change of ice sheet volume when $dL/dt < 0$ (sea cooling effect) and that the mass lost to iceberg calving is proportional to the rise in sea level once an ice sheet that is larger than some critical size begins to melt. The rise in sea level is proportional to the difference between the maximum ice sheet volume V_{max} and its volume V at the time under consideration.

More specifically, we include the two effects in the ice sheet model by first writing the net volume accumulation rate as

$$\int_0^L g(y)\,dy = A_1 + A_2, \tag{13}$$

where A_1 is the positive part of the integral (the gross accumulation rate) and A_2 is the negative part (the gross ablation rate). In the numerical computation, whenever $dL/dt < 0$, i.e., the ice sheet is melting, a new expression for the gross accumulation rate is used. The new value, A_1', is

$$A_1' = A_1 \left[1 + K_1 \frac{d}{dt}([1 + \eta] R^3)\right]. \tag{14}$$

If a negative value is predicted for A_1', A_1' is set equal to zero. The quantity $(1 + \eta) R^3$ is proportional to the ice sheet volume. Similarly, when the ice sheet volume is decreasing, and, in addition, $(1 + \eta) R^3$ has exceeded $10^6\ m^{3/2}$, a new expression, A_2', is used instead of A_2 for the gross ablation rate of the ice sheet. The new value is

$$A_2' = A_2 - K_2\{[(1 + \eta) R^3]_{max} - (1 + \eta) R^3\}. \tag{15}$$

The values of K_1 and K_2 are chosen so that when the ice sheet model is run with the climate point variation taken from the seasonal climate model, the Northern Hemisphere ice sheets from the most recent glaciation disappear completely by the present time. The values used in this paper are $K_1 = 10^5\ m^{-3/2}$ and $K_2 = 1.1 \times 10^{-4}\ m^{1/2}\ yr^{-1}$. (One model run for $K_1 = K_2 = 0$ is included in Fig. 6 to facilitate later discussion.) The actual rate of volume decrease due to iceberg calving predicted by the ice sheet model never exceeds $10^3\ km^3$/year. This value is modest compared with that used by Pollard (1982).

5. How the climate and ice sheet models are combined

In this section we outline the procedure that was used to combine the climate and ice sheet models, and thereby to test the Milankovitch hypothesis. We have already suggested that if a climate model is to have a chance of providing a test of the Milankovitch hypothesis, it must have, at least, a seasonal cycle, a separate treatment of continental and oceanic regions, and an interactive ice sheet model. The climate model described in Section 2 is probably the simplest possible model that contains these effects. Nevertheless, the climate model calculations are so time consuming that it is not practical to run it simultaneously with the ice sheet model for one or more glacial cycles, i.e., for 150,000 to 250,000 years. It was therefore necessary to devise a way to use the climate model to estimate the variations in the climate point over the past few hundred thousand years, and then to use the climate point variation within the ice sheet model to predict the variation in the ice sheet size.

The climate point is the point of intersection of the equilibrium line with the earth's surface at mean sea level. If the climate point remains on the continent during the entire year, snow and ice can accumulate. The furthest (seasonally) poleward point of the snow line at $\phi = 0$ (mid-continent) was estimated using the climate model and was assumed to be the climate point. Strategic time periods were chosen by examining radiation data calculated using the formulae given by Berger (1978), and the climate point location was determined 23 times during the past 240,000 years. The results are shown in Fig. 4 as open circles. According to our model, the climate point is presently located at about 70 km north of the northern edge of the central continent and therefore does not lie on the continent.

In order to run the ice sheet model, it was desirable to have a smooth representation of $P(t)$. The values of $QS(x, t)$ at particular latitudes were computed over the last 250,000 years using the formulae given by Berger (1978) and their shapes were compared with Fig. 4. The smooth curve in Fig. 4 shows a linear function of the variation of the $QS(x, t)$ at 73° N. Its shape is very similar to the values of $P(t)$ obtained from the climate model. The

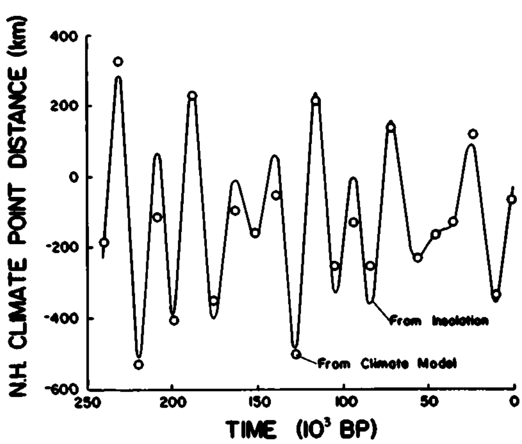

Fig. 4. Variation of the climate point.

smooth curve was actually used as $P(t)$ in the ice sheet model.

Once the climate point variation has been determined and the ice sheet model has been used to find the variation in ice sheet size, the seasonal cycle for any given year can be found by inserting an ice sheet of the proper size into the seasonal model and running the climate model again. This has been done in order to estimate the variations in the sea ice extent and ocean temperature for comparison with the paleoclimatic record.

There is a potential problem in this scheme. The climate point is determined using a seasonal climate model without an ice sheet present. If a large ice sheet were present throughout the year, the location of the climate point might not be the same because the presence of the ice sheet introduces two additional opposing feedbacks: ice co-albedo feedback and height infrared radiation feedback. The climate model contained seasonally variable snow co-albedo feedback, but not ice co-albedo feedback. When an ice sheet is present, it remains fixed in size during the seasonal cycle. It extends considerably further equatorward than the climate point, especially during the summer. The lower co-albedo of the ice cap compared to the base surface (when snow is absent) tends to cool down the climate, and therefore to shift P equatorwards (a positive feedback). The surface area under an icecap varies nearly linearly with the length of the ice sheet, so the ice co-albedo feedback might be expected to respond more or less linearly with the ice sheet length. The increased height of the ice surface, on the other hand, lowers the surface temperature, and therefore the infrared radiation leaving the system, making the climate warmer (a negative feedback). This effect has been studied by Bowman (1982) using an annual mean energy balance climate model. He found the effect to be substantial. The average height of the ice sheet is proportional to the square root of ice sheet length. Therefore, this feedback is expected to vary approximately as the square root of the ice sheet length. The effect of these feedbacks was examined at two different times in the past by inserting ice sheets of various sizes into the climate model at these times and determining the resulting shift in the climate point. The results are shown in Fig. 5. The ice sheet feedback is negative when the ice sheet is small because the height infrared radiation effect is the larger of the two feedbacks. For larger ice sheets, however, the feedback becomes positive because the ice co-albedo feedback increases faster than the height infrared radiation effect.

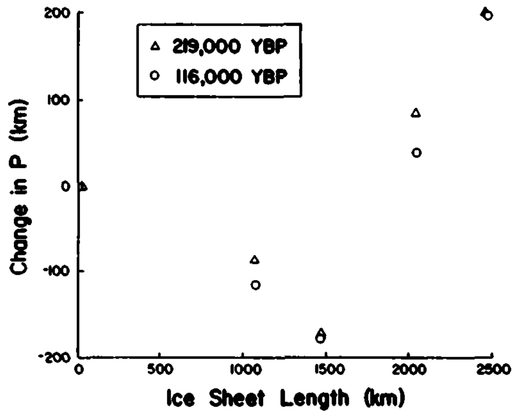

Fig. 5. Variation of the climate point with ice sheet length: ice sheet feedback.

It is clear from Fig. 5 that these two feedbacks can be important. While we intend to incorporate them in a more detailed model in the future, we decided to neglect these effects in the present study. In the next section we shall point out why they may not be as important as Fig. 5 might at first lead one to believe.

6. The last two glacial cycles

Using the climate point variation shown in Fig. 4, the ice sheet model was run for the last two glacial cycles. The constants used in the model are shown in Table 2. The values of a and b are about 35% higher than those used by Oerlemans (1980) and slightly higher than those used by Pollard (1982). The accumulation expression used by Weertman (1976) is somewhat different, so a direct comparison is not possible. However, our values of

Table 2. *Constants used in the ice sheet model*

γ	14 m
a	$0.98 \times 10^{-3}\ yr^{-1}$
b	$0.36 \times 10^{-6}\ m^{-1}\ yr^{-1}$
s	10^{-3}
α	$2 \times 10^{-4}\ yr^{-1}$
K_1	$10^{-5}\ m^{-3/2}$
K_2	$1.1 \times 10^{-4}\ m^{1/2}\ yr^{-1}$

average accumulation and ablation rates are substantially smaller than Weertman's. The slope of the equilibrium line was calculated in the climate model. The value of this important parameter varied with both latitude and season. The seasonal variation, especially, could be of considerable importance. In keeping with other simplifications, we have used an average value of approximately 0.001 in this study.

The quantity $(1 + \eta) L^{3/2}$, which is proportional to ice sheet volume, and the mid-continent ice sheet length variations for the past 240,000 years are shown in Figs. 6 and 7. Oxygen isotope data, redrawn from Emiliani (1978), is shown for qualitative comparison with the ice volume curve. The predicted ice sheet size is quite large, extending equatorward as far as 45° N at times, with a pronounced periodicity near 100,000 years and a smaller one at approximately 40,000 years.

A disturbing feature of the model is its sensitivity to K_1 and K_2. We found that a small increase in either K_1 or K_2 causes the ice sheet to collapse prematurely, whereas a small decrease results in an ice sheet that does not disappear completely during periods of known interglacials. The case in which $K_1 = K_2 = 0$ (i.e. no enhanced melting) is shown in Fig. 6 for comparison. There is essentially no 100,000 year periodicity in this curve. Nevertheless, it is clear that the model can produce very large glacial cycles with periodicities that agree roughly with those deduced from oxygen isotope data when it is forced by insolation changes resulting from orbital variations and when some collapse mechanism is included in the ice sheet model. The model is at least partially coupled with a climate model in the sense that the climate point variations are calculated using a seasonal climate model.

A significant and interesting feature of the ice sheet model is that ice sheets with a latitudinal extent reaching $2L \sim 2700$ km can be produced when P has a maximum value of only about 200 km. This point has been discussed by Oerlemans (1981). When $P = 0$, there are two possible real steady state solutions of Eq. (12). One solution is $L = 0$, and the other gives a very large ice sheet. The physical reason for the large L solution is that, once an ice sheet begins to grow, its upper surface extends above the equilibrium line (see Fig. 3), increasing the area over which mass can accumulate. The ablation rate on the equatorward end of the ice sheet also increases, of course, as the ice sheet extends further equatorward, and this eventually causes the ice sheet to stop growing, but not before a very large ice sheet is formed. This is a crucial point. It is the reason why an ice sheet must be used (in conjunction with a seasonal climate model) in investigating the Milankovitch hypothesis. Without the presence of the ice sheet, only the variation in P could be predicted by a climate model. This is what was done by North et al. (1982). If an ice sheet is not present, the climate signal that results from the orbital parameter variations is simply the variation in the equatorward extent of the region in which temperatures never exceed freezing.

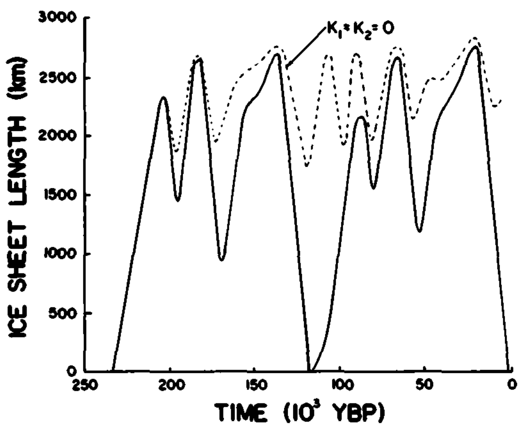

Fig. 6. Predicted ice sheet length during the past 240,000 years.

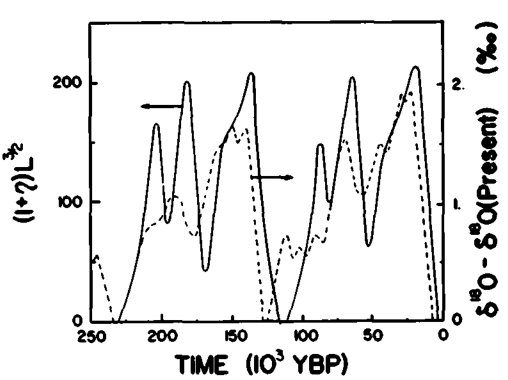

Fig. 7. Predicted ice volume and the data of Emiliani (1978).

The size of the large ice sheet is only weakly dependent on the size of P if $P \geqslant 0$, as shown by Oerlemans (1981). It is quite likely, therefore, that the effects of the height infrared radiation and the ice co-albedo feedbacks discussed in Section 5 are somewhat less important than they might at first appear to be. If the climate point moves onto the continent, the ice sheet grows quite rapidly, even if P is small. Also, once the ice sheet becomes large it is not completely destroyed even when the climate point periodically moves far off the continent, unless some additional collapse mechanism is introduced. The dashed line in Fig. 6 shows the solution that we obtained with $K_1 = K_2 = 0$. Similar results have been reported by Pollard (1982). Some mechanism that enhances the collapse of large ice sheets is necessary in our model, and in models like it, if a large 100 kyr cycle in the ice sheet size is to be produced.

7. The climate during an ice age

Seasonal climate model results were computed using a climate model that contained the ice sheet taken from the results of the ice sheet model. In this way we determined the seasonal temperature distribution at various times in the past. In the climate model, the snow line was allowed to vary with season, but the boundary of the land ice sheet was kept fixed throughout any given year.

A comparison of the computed temperature distributions for the Northern Hemisphere summer and winter 23,000 YBP (at a peak ice sheet size) with those computed for the present is shown in Figs. 8 and 9. Computed summer temperatures along the centerline of the Northern Hemisphere continent are at most only 2 °C to 3 °C cooler 23,000 YBP. Mid-ocean temperature differences are even smaller. Northern latitude winter temperatures were very slightly *warmer* than those of today. This is logical. The orbital parameters 23,000 YBP were in fact very similar to those of today. During the winter, when the snow line is farther equatorward than the ice sheet, the ice age increase in the ice-albedo effect is minimal, while the ice sheet height infrared feedback is strong.

A similar calculation has been made at 11,000 YBP. The detailed results are given by Hayder (1982). The differences between the 11,000 YBP and the 23,000 YBP results are more pronounced than those shown in Figs. 8 and 9 because the differences in the orbital parameters are larger. Northern Hemisphere mid-continent summer temperature differences are about twice as large. Although the Northern Hemisphere summer is warmer at 11,000 YBP, the winter is actually colder than the 23,000 YBP winter. This is because the orbital parameters are such that the Northern Hemisphere winter insolation is larger at 23,000 YBP.

Note that the ocean remains ice free up to latitudes far poleward of the ice sheet limit, especially during summer. This has apparently been the case during the Pleistocene glaciations, except during the rapid termination phases. Ruddiman and McIntyre (1981) used microfossil evidence from deep ocean cores to estimate temperature variations in the central North Atlantic Ocean during the past 200,000 years. They concluded that during ice sheet melting the ocean

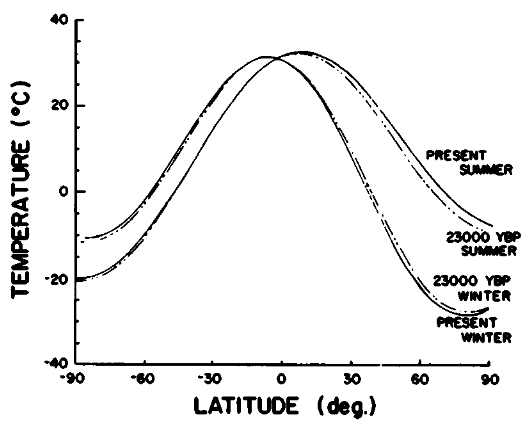

Fig. 8. Comparison of the model's present climate with that at peak glaciation: mid-continent.

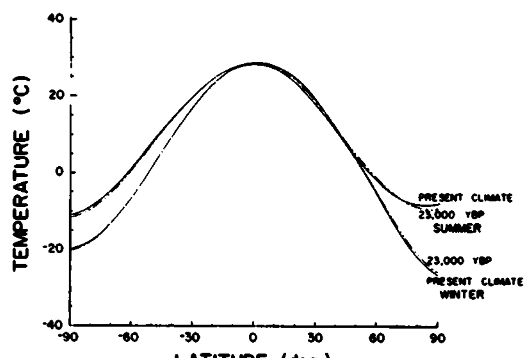

Fig. 9. Comparison of the model's present climate with that at peak glaciation: mid-ocean.

surface temperature decreased at certain times by 5–10 °C in the mid-latitude North Atlantic. We have attempted to reproduce the effect of a cooling caused by deglacial meltwater with our climate model. As we explained in Section 2, the sea cooling effect is concentrated within a portion of the ocean between 40° N and 55° N. Even so, the ocean surface temperature fluctuations computed are quite small (Fig. 9). First of all, the diffusivity of heat in the model is large enough that any local temperature decrease is spread out over the ocean on a time scale much smaller than the time scale of the melting of the ice sheet. Perhaps a more important point is that the thermal relaxation time of the system is also small relative to the 5000 to 10,000 years required to melt a large portion of land ice. Any decrease in the ocean surface temperature would decrease the infrared radiation term in the energy equation and the resulting radiation imbalance would tend to increase the ocean surface temperature. The direct effect of meltwater and iceberg melting in the sea is probably quite small. As suggested by Ruddiman and McIntyre (1981), the effect is more likely indirect. We offer here one possible explanation.

When a large amount of relatively fresh meltwater is introduced into the ocean it will tend (as pointed out by Ruddiman and McIntyre (1981)) to remain in the mixed layer. One would expect this meltwater to inhibit the sinking of water in the high latitude North Atlantic. The resulting decrease in deep ocean turnover might, among other things, cause a redistribution in the temperatures of the mixed layer and the bottom water such that the temperature of high- and mid-latitude surface water would decrease, while equatorial water temperature would increase very slightly. (See, for example, Sverdrup; 1940). We are presently exploring a simple model of this effect using a very simple deep ocean model. The phenomena may be especially important for climate fluctuations with periods between 100 years and 2000 years (Schnitker, 1983).

8. Conclusions

We summarize our conclusions as follows:

1. A climate model with seasons is necessary in testing the Milankovitch theory of ice ages because that theory asserts that ice sheet growth is initiated when a region of below freezing temperatures persists on a continent throughout the year.

2. Realistic distributions of land and sea should be included in the climate model because these distributions affect the seasonal fluctuation of the temperature field.

3. If a portion of the land surface remains below freezing during the entire year we assume that snow accumulates there, that an ice sheet forms and that the ice sheet flows like a perfectly plastic substance (Weertman, 1976). The fact that the ice sheet extends high into the atmosphere, where temperatures are cooler, allows a larger portion of its surface to experience net snow accumulation. The result is that an ice sheet can grow to be very large even if the portion of the land surface (in the absence of the ice sheet) that remains below freezing is small. Thus, the ice sheet model itself must be an integral part of any attempt to test the Milankovitch theory.

4. While our ice sheet model was driven by a signal essentially like one produced by our climate model, it was not explicitly contained within the climate model. This eliminated two potentially important feedbacks: the ice co-albedo feedback and the height infrared radiation feedback. These feedbacks were briefly explored in Section 5. They essentially modulate the value of P, the climate point distance. Since the size of the ice sheet is not strongly dependent on the magnitude of P (as long as $P > 0$ for a long enough time) we feel that including these feedbacks would not greatly affect our results. Nevertheless, these effects should be studied in the future.

5. Finally, our results imply, as do the results of Oerlemans (1981), that once a large ice sheet is present even very large negative values of the climate point do not cause the ice sheet to completely disappear. Some additional mechanism must be responsible for the rapid collapse of the ice sheet. We have postulated, and very crudely parameterized, an iceberg calving mechanism that does indeed produce the complete collapse of our model ice sheet. When this mechanism is added to our ice sheet model, variations in ice volume similar to those that occurred during the past 240 kyr are predicted.

9. Acknowledgements

This research was supported by The National Science Foundation under Grant ATM 79/16332 at Tulane University.

REFERENCES

Barron, E. J., Thompson, S. L. and Schneider, S. H. 1981. An ice-free Cretacious? Results from model studies. *Science 212*, 501–508.

Berger, A. L. 1978. Long term variations of daily insolation and quaternary climatic changes. *J. Atmos. Sci. 35*, 2363–2367.

Birchfield, G. E. 1977. A study of the stability of a model continental ice sheet subject to periodic variation in heat input. *J. Geophys. Res. 82*, 4909–4913.

Birchfield, G. E., Weertman, J. and Lunde, A. T. 1981. A paleoclimate model of northern hemisphere ice sheets. *Quaternary Res. 15*, 126–142.

Bowman, K. P. 1982. Sensitivity of an annual mean diffusive energy balance model with an ice sheet. *J. Geophys. Res. 87*, 9667–9674.

Budyko, M. I. 1969. The effect of solar radiation variation on the climate of the earth. *Tellus 21*, 611–619.

Burrett, C. F. 1982. Phanerozoic land–sea and albedo variations as climate controls. *Nature 296*, 54–56.

Emiliani, C. A. 1978. The cause of the ice ages. *Earth and Planet. Sci. Lett. 37*, 349–352.

Hayder, Md. E. 1982. A two-dimensional, seasonal, energy balance climate model with continents and ice sheets: Testing the Milankovitch theory of ice ages, M.S. Thesis, Mechanical Engineering, Tulane University.

Hays, J. D., Imbrie, J. and Shackleton, N. J. 1976. Variation in the earth's orbit: Pacemaker of the ice ages. *Science 194*, 1121–1132.

Kukla, G. J. 1978. Recent changes in snow and ice. In: *Climatic change* (ed. John Gribbin). Cambridge Univ. Press, 114–129.

Mayewski, P. A., Denton, G. H. and Hughes, T. J. 1981. Late Wisconsin ice sheets in North America. In: *The last great ice sheets* (ed. G. H. Denton and T. J. Hughes). Wiley Interscience, 67–170.

Milankovitch, M. 1941. Canon of insolation and the ice age problem. Belgrade: Royal Serbian Academy. Special Publication 133, 482 pp. Translated by Israel Program for Scientific Translation, Jerusalem, 1969.

North, G. R. 1975. Analytical solution to a simple climate model with diffusive heat transport. *J. Atmos. Sci. 32*, 1301–1307.

North, G. R., Cahalan, R. F. and Coakley, J. A. 1981. Energy-balance climate models. *Rev. Geophys. Space Phys. 19*, 91–121.

North, G. R. and Coakley, J. A. 1979. Differences between seasonal and mean annual energy balance model calculations of climate and climate sensitivity. *J. Atmos. Sci. 36*, 1189–1204.

North, G. R., Mengel, J. G. and Short, D. A. 1982. Continentality and the Milankovitch theory of the ice ages: Experiments with a simple model. Presented at the G.S.A. 1982 Spring Meeting, Philadelphia, May 31–June 4, 1982.

Oerlemans, J. 1980. Model experiments on the 100,000-yr. glacial cycle. *Nature 287*, 430–432.

Oerlemans, J. 1981. Some basic experiments with a vertically-integrated ice sheet model. *Tellus 33*, 1–11.

Pollard, D. 1982. A simple ice sheet model yields realistic 100 kyr glacial cycles. *Nature 296*, 334–338.

Pollard, D., Ingersoll, A. D. and Lockwood, J. L. 1980. Response of a zonal climate ice sheet model to the orbital perturbations during the quaternary ice ages. *Tellus 32*, 301–319.

Ruddiman, W. F. and McIntyre, A. 1981. Oceanic mechanisms for amplification of 23,000 year ice volume cycle. *Science 212*, 617–627.

Schnitker, D. 1983. Climate variability and deep ocean circulation: Evidence from the North Atlantic. *Paleogeography, Paleoclimatology, and Paleoecology*, accepted for publication.

Suarez, M. J. and Held, I. M. 1979. The sensitivity of an energy balance climate model to variations in the orbital parameters. *J. Geophys. Res. 84*, 4825–4836.

Sverdrup, H. V. 1939. Lateral mixing in the deep water of the South Atlantic Ocean. *J. Mar. Res. 2*, 195–207.

Tanner, W. F. 1968. Cause and development of an ice age. *Meterol. Monogr. 8*, 126–127.

Weertman, J. 1976. Milankovitch solar radiation variations and ice-age ice-sheet sizes *Nature 261*, 17–20.

Winston, J. S., Gruber, A., Gary, T., Varnadore, M., Earnest, C. and Annello, L. M. 1979. *Earth-atmosphere radiation budget analysis derived from NOAA satellite data—June 1974–February 1978*, Vol. 1. U.S. Department of Commerce.